INTEGRATED CONTROL LAW SYNTHESIS OF GUST LOAD ALLEVIATION AND FLUTTER MARGIN AUGMENTATION FOR A TRANSPORT AIRCRAFT

ICAS-92-5.5.2

H. Matsushita*, K. Fujii** and Y. Miyazawa †
National Aerospace Laboratory
Tokyo, Japan

Abstract

In this paper an integrated synthesis method of gust load alleviation control laws for a flexible aircraft which can also guarantee flutter margin augmentation is presented.

The method is applied to a wind tunnel test model which has both aeroelastic and dynamic similarity. A mathematical model is derived in a state space time domain based on the FEM structural analysis and the boundary element unsteady aerodynamic analysis. The math model is tuned to be consistent with ground vibration and wind tunnel test results.

Based on this math model, control laws are synthesized applying the Linear-Quadratic-Gaussian (LQG) optimal control law synthesis method with an order reduction procedure at design speeds of both a subcritical and a supercritical flutter state. With a cost function of a model's kinetic energy to be minimized, control laws obtained satisfy the design requirement of gust load alleviation and flutter margin augmentation.

Typical control laws obtained were implemented in a digital computer and tested in the 6.5m X 5.5m subsonic wind tunnel at the National Aerospace Laboratory and analytically predicted results to alleviate gust loads and augment a flutter speed were verified in the tests.

1. Introduction

Experimental and analytical studies on active control technology (ACT) for aeroelastic systems have been persistently pursued at the National Aerospace Laboratory (NAL), with previous work focusing on cantilevered wing models.[1]-[9] These investigations were extended to include a complete aircraft model having a high aspect-ratio wing with aeroelastic similarity.[10]

A mathematical aircraft model was derived in a state space form, and was tuned to be consistent with ground vibration and wind tunnel tests. In this model, heaving, pitching and wing vibration were taken into account. The Linear Quadratic Gaussian (LQG) optimal control synthesis method was then applied to the model, with Hyland's method additionally incorporated so as to obtain practical low order control laws.[11]

Typical control laws derived were served in wind tunnel tests that utilized a newly developed active suspension system. This system enabled the aircraft model to fly in the wind tunnel and have freedom in heaving, yawing, and pitching. The NAL Low-Speed Wind Tunnel (6.5m X 5.5m) was used for these tests.

Analytical and experimental results showed that the wing's acceleration feedback plays an essential role in reducing the wing root bending moment, and also that the addition of bending strain feedback further reduces this bending moment, especially in the rigid-body mode frequency range. In addition, the elevator was found to slightly improve control performance.

For practical application of gust load alleviation system it is necessary not to sacrifice the flutter margin. Although there were many investigations on the simultaneous fulfillment of gust load alleviation and active flutter suppression,[12],[13] integrated design method which incorporates an efficient order reduction method is not yet established. Recently the last author of the present paper proposed the multiple model approach as a robust control design method.[14],[15] As an application of this approach, multiple design point approach combined with Hyland's order reduction method is proposed here for an integrated design method for gust load alleviation and flutter margin augmentation.

2. ACT Wind Tunnel Test Model

A scaled transport aircraft model which was designed and constructed for wind tunnel tests has aspect ratio of 9.86, swept back angle of 18°, and its wings have an aeroelastic similarity to a particular future transport aircraft. The ailerons are driven by electric DC servo-motors, and the elevator is driven by a stepping motor, with both being utilized as control devices. The horizontal tail and rudder are activated for pitch and yaw trim, respectively. Systematic diagram of the ACT (Active Control Technology) model is depicted in Figure 1.

Figure 2 shows the wind tunnel test set-up, with the model being supported by a vertical rod which allows it to go up and down along the rod. Pitch and yaw freedom are also given. Since the model lift is not enough at trim speed, two cables having their tension controlled by a torque motor are attached onto the wind tunnel test section. A gust generating system is additionally attached upstream on the test section wall.

3. Aeroservoelastic Math Model

3.1 State-Space Equations of Motion

A mathematical aircraft model is obtained in a state space form. The wing deflections are treated using a modal approach. The finite element method (FEM) is used to extract five natural modes which approximate the wing motion in the response analysis, being tuned so as to be consistent with the ground vibration test results. The wing deflections, $z(x,y,t)$, can be expressed with N natural modes, $z_{ai}(x,y)$, as

$$z(x,y,t) = \sum_{i=1}^{N} z_{ai}(x,y) q_i(t) \tag{1}$$

using the generalized coordinates $q_i(t)$.

The linearized equations of motion for heaving and pitching degree of freedom are

$$m\ddot{h} = L_\alpha \alpha + L_{\dot\alpha}\dot\alpha + L_q q + \sum_{i=1}^{N} (L_{qi} q_i + L_{\dot qi}\dot q_i) + L_\alpha \alpha_g + L_{\delta a}\delta_a + L_{\delta e}\delta_e \tag{2a}$$

$$I_y\ddot\theta = M_\alpha \alpha + M_{\dot\alpha}\dot\alpha + M_q q + \sum_{i=1}^{N} (M_{qi} q_i + M_{\dot qi}\dot q_i) + M_\alpha \alpha_g + M_{\delta a}\delta_a + M_{\delta e}\delta_e \tag{2b}$$

where m and Iy are the model's mass and moment of inertia, respectively. $\alpha = \theta - \dot h/U_0$ is an angle of attack, q is pitch rate, α_g is gust incidence and $\delta a/\delta e$ the aileron/elevator deflections.

---

* Deputy Director, Advanced Aircraft Research Group
** Researcher, Advanced Aircraft Research Group
† Head, Flight Analysis Branch, Flight Research Division

L_α's and M_α's are quasi-steady aerodynamic coefficients. The equations for a wing vibration can be expressed for each natural mode as

$$\ddot{q}_j + 2\xi_j\omega_j\dot{q}_j + \omega_j^2 q_j + s_{aj}\delta_a = f_{\alpha j}\alpha + \sum_{i=1}^{N}(f_{qji}q_i + f_{\dot{q}ji}\dot{q}_i) + f_{\alpha j}\dot{\alpha} + f_{\delta j}\dot{\delta}_a \quad (2c)$$

ω_i, ξ_i and the aileron's inertial coupling coefficient s_i are obtained by ground vibration tests. The generalized aerodynamic forces on the right hand side of Eq. (2c) are estimated by the boundary element unsteady aerodynamic analysis and can be expressed by the aerodynamic lag using the supplementary variables r as

$$\begin{aligned} f(t) &= A_2\ddot{q}(t) + A_1\dot{q}(t) + A_0 q(t) + r(t) \\ \dot{r}(t) &= Fr(t) + Gq(t) \end{aligned} \quad (3)$$

where $q = (q_1\, q_2 \ldots q_N)^T$, $F = diag(-\lambda, \cdots, -\lambda)$

Other equations are for the control surface actuating system and gust generating system. Aileron/elevator actuating systems are expressed in the form of second order dynamic systems; a first order shaping filter is included to express a gust model.

The governing equations are eventually written in the form of a state space model as

$$\dot{x}(t) = Ax(t) + Bu(t) + w(t) \quad (4a)$$

where $x = (h, \theta, \dot{q}, \delta a, \delta e, h, \theta, q, \delta a, \delta e, r, \alpha g)$. Components of u are the control commands to the aileron and elevator actuating systems, and w represents the white noise which is input to the gust model shaping filter. The output equations which estimate the fore/aft body and wing vertical accelerations, wing bending and torsional strains, pitch angle, and vertical deflection are expressed as

$$y(t) = Cx(t) + Du(t) + v(t) \quad (4b)$$

with v being a measurement noise.

3.2 Simmetrization of a Math Model

In the ground vibration tests previously executed, asymmetry in the torsional natural modes was observed, being caused by torsional elasticity differences between the wings. If the mathematical model accounts for these differences in elasticity, the left and right wing torsion natural modes appear independently of each other. Since it is assumed the aircraft model has symmetric motion, a math model is simmetrized by applying the resulting left wing torsional elasticity to the right wing.

Two mathematical models are subsequently obtained. The one is a sophisticated model, which can predict precisely the aircraft model's dynamics by expressing the wing deflections with five natural modes. They are three bending modes, asymmetric left and right wing torsional modes. This asymmetric model has an order of 24. The other is a symmetric model of 18-order, and expresses the wing deflection with three natural modes; two bending modes and a symmetrized torsional mode (Fig.3). Comparison of the velocity root loci (Figs. 4a,b) of both models indicate that the first order bending mode, which is essential to gust load alleviation, and flutter characteristics are as well expressed by a symmetrical model as a sophisticated model. The frequency responses also show good correspondence to the experimental results. The LQG optimal control synthesis method is applied to the symmetric math model, accordingly. The sophisticated model is used to evaluate the control law performance prior to the experiments.

4. GLA/FMA Control Law Synthesis

4.1 GLA Controller

The present control law synthesis procedure is based on LQG control theory. The first step of the procedure is to derive a full-state feedback control. The cost function, J, is defined as

$$J = E(1/2\, x^T Q x + 1/2\, u^T R u) \quad (5)$$

where the first term in the brackets represents the kinetic energy, R in the second term represents control weights, and E( ) indicates an average value. Since a model cruising speed is 25 m/s, design velocity for GLA controller is set there at 25 m/s. With the aileron/elevator control weights as parameters, optimal regulator is obtained by solving the Riccati equation. Following this, a diagram showing trade-off between control deflections and energy reduction is obtained as in Figure 5. The design weight of 15/15 for aileron/elevator is selected so that moderate values of control deflections result at certain level of gust load alleviation measured by the elastic energy reduction ratio.

The next step of control law synthesis is to design a state observer applying a Kalman estimator with wing accelerometers and/or wing strain as inputs. The resulting full-order output control laws have an order of 18, the same order as the math model. Since the full 18-order output control laws are too large for real time computation, Hyland's method[11] is introduced for order reduction.

Table 1 contains the performance of two sets of control laws obtained (A1, A2). A full-state controller derived with a control weight of 15 reduces the elastic energy to 49%. Corresponding full order controller using the wing accelerometer reduces the elastic energy to 51%, slightly degraded the full state controller. Based on this control law, a lower order controller (order 4) is obtained using Hyland's order reduction method, where the energy reduction ratio is further degraded to 58%.

This reduced order controller is evaluated for frequency response as in Figure 6(1). This figure shows that controls can alleviate both acceleration and bending moment response almost all the frequency range except the lowest resonance region for bending strain; though acceleration is suppressed in this region, bending strain is increased instead. Intending to improve this deficiency, strain signal is included as a feedback signal along with acceleration. Resulting low order controller (order 2) shows expected improvement in performance as in Figure 6(2) and A2 control law in Table 1.

Since the cost function used to synthesize the gust load alleviation control laws is the aircraft model's kinetic energy, control laws should be effective for flutter suppression as well. Table 1 shows that each control law, even designed at a subcritical speed, shows a certain level of flutter margin augmentation.

4.2 Wind Tunnel Test Verification

Practical performance of these two types of control laws were investigated in wind tunnel tests.[10] Test frequency responses are summarized in Fig. 7 (1), (2). Wind tunnel tests were also executed at different wind speeds from which flutter stability margin was extracted by the NAL's AR model identification technique. Figure 8 shows the results where the analytical results in Table 1 are confirmed. Since the correspondence between analysis and experiment shown in Figs. 6, 7 and Table 1 is fairly good, it is confirmed that the present control law synthesis method is effective for gust load alleviation with a certain level of flutter margin.

4.3 GLA/FMA Controller

In order to enhance flutter margin augmentation, an intentional use of the cost function to increase a flutter speed was intended; design velocity was set equal to 33m/s, being higher than the model's estimated flutter speed (supercritical speed). In order to get the control laws with the same level of control surface activation, the control weights were adjusted lower than the design values at 25 m/s. With the control weights of 400/15 for aileron/elevator, improved GLA/FMA controller were able to be obtained as shown as control law B in Table 1 where the higher flutter margins are attained than by control laws designed at 25 m/s.[17]

Further improvement of the control law are tried by introducing the multiple design point approach. Since the coefficients of the plant equations (4a), (4b) depend on a velocity, equations at two different design speeds can be expressed as,

$$\begin{aligned} x_i(t) &= A_i x_i(t) + B_i u_i(t) + w_i(t) \\ y_i(t) &= C_i x_i(t) + D_i u_i(t) + v_i(t) \end{aligned} \tag{6}$$

where i=1 for supercritical speed and i=2 for subcritical speed. Control law to be designed is a reduced order controller and has the following common structure for different speeds.

$$\begin{aligned} p(t) &= Fp(t) + Gy_i(t) \\ u_i(t) &= Hp(t) \end{aligned} \tag{7}$$

In this case performance index J to be optimized is defined both at subcritical and supercritical speed simultaneously as follows.

$$J = \sum_{i=1}^{N} p_i J_i \tag{8}$$

where $J_i = E(1/2\, x_i^T Q x_i + 1/2\, u_i^T R u_i)$ (9)

J_i is the cost function for each model similar to that of an ordinary LQG problem. $p_i(>0)$ is a weight for i-th model satisfying $p_1 + p_2 = 1$, and is design parameters. The problem can be stated to seek the matrices F, G, H so as to minimize the performance index J under the constraint of Eq. (6).
As a minimization algorithm, a quasi-Newton method of Fletcher[16] may be used. Since a reduced order optimal control law at a supercritical speed has already obtained as a control law B, it can be used as an initial values for the multiple design point problem.

As an example of applying the present method, it is assumed that only the components of F matrix in a controller are optimized parameters, while, the other components in G and H matrix are fixed. By choosing p_1 equals to 0.25 and p_2 to 0.75, we were able to obtain a control law which refine the performance index at a cruising speed of 25 m/s as shown as control law C in Table 1 and in Figure 10. Though the energy reduction ratio at 25 m/s is moderated, the control surface movements are remarkably reduced there.

5.Conclusions

A mathematical model for an aeroservoelastic system is developed to adequately determine the dynamics of a flexible transport aircraft. The math model is derived in the state space time domain based on the FEM structural analysis and the boundary element unsteady aerodynamic analysis.

An integrated control law synthesis method which can realize gust load alleviation and flutter margin augmentation simultaneously is proposed. The synthesis method comprises the LQG optimal control law design procedure with the order reduction method applied at the design speeds of both the sub- and super-critical flutter state.

Typical control laws obtained were implemented in the wind tunnel test and test results confirmed the analytically predicted results, so that the effectiveness of the proposed synthesis method was verified.

References

(1) Matsushita, H., "Active Aeroelastic Control - Research Status in NAL," *Journal of the Japan Society for Aeronautical and Space Sciences*, Vol. 35, No.3, 1987, in Japanese.
(2) Matsushita, H. and Matsuzaki, Y., "Research Activities on Aircraft Control Technology of Aircraft in Japan," Proceedings of the International Symposium on Active Materials and Adaptive Structures, Alexandria, U.S.A., Nov. 4-8, 1991.
(3) Matsuzaki, Y., Ueda, T., Miyazawa, Y. and Matsushita, H., "Gust Load Alleviation of a Transport-type Wing: Test and Analysis," *Journal of Aircraft*, Vol. 26, April 1989, pp.322-327.
(4) Ueda, T., Matsushita, H., Suzuki, S. Miyazawa, Y. and Matsuzaki, Y., "ACT Wind Tunnel Experiments of a Transport-type Wing," ICAS '88, Israel, Aug. 28 - Sept. 2, 1988, also as *Journal of Aircraft*, Vol.28, Feb. 1991, pp.139-145.
(5) ACT Study Group, "Gust Load Alleviation of a Cantilevered Rectangular Elastic Wing. -- Wind Tunnel Experiment and Analysis." NAL TR-846. 1984, in Japanese.
(6) ACT Study Group, "Wind Tunnel Tests and Analysis on Gust Load Alleviation of a High-Aspect-Ratio Wing," NAL TR-890, 1985, in Japanese.
(7) ACT Study Group, "Wind Tunnel Tests on Flutter Control of a High-Aspect-Ratio Cantilevered Wing, 1st Report," NAL TR-978, 1988, in Japanese.
(8) Matsushita, H., Miyazawa, Y., Ueda, T. and Suzuki, S., "Multi-Surface Control Law Synthesis and Wind Tunnel Test Verification of Active Flutter Suppression for a Transport-type Wing," Proceedings of the European Forum on Aeroelasticity and Structural Dynamics, Aachen, FRG, April 17-19, 1989, pp.519-527.
(9) ACT Study Group, "Wind Tunnel Tests on Flutter Control of a High-Aspect-Ratio Cantilevered Wing, 2nd Report," NAL TR-1070, 1990, in Japanese.
(10) Matsushita, H., Ueda, T., et al, "Control Law Synthesis and Wind Tunnel Test of Gust Load Alleviation for a Transport-type Aircraft," ICAS '90, Sweden, Sept. 10-14, 1990.
(11) Greeley, S. W. and Hyland, D. C., "Reduced-Order Compensation: Linear-Quadratic Reduction Versus Optimal Projection," *Journal of Guidance, Control, and Dynamics*, Vol. 11, No.4, 1988, pp.328-335.
(12) Gangsaas, D, Ly, U. and Norman, D.C., "Practical Gust Load Alleviation and Flutter Suppression Control Laws Based on a LQG Methodology," AIAA 19th Aerospace Sciences Meeting, St. Louis, U.S.A., Jan. 12-15,1981.
(13) Karpel, M., "Design for Active Flutter Suppression and Gust Alleviation using state-space aeroelastic Modeling," Journal of Aircraft, vol.19, March 1982, pp.221-227.
(14) Miyazawa,Y., "Robust Control System Design with Multiple Model Approach and Its Application to Active Flutter Control," AIAA Guidance, Navigation and Control Conference, Boston, U.S.A., August 14-16, 1989.
(15) Miyazawa, Y., "Robust Control System Design with Multiple Model Approach and Its Application to Flight Control System," ICAS-90-5.6.1, ICAS'90, Stockholm, Sweden, Sept. 10-14, 1990.
(16) Fletcher, R., "FORTRAN Subroutines for Minimization by quasi-Newton Method," Report R7125 AERE, Harwell, England, 1972.
(17) Fujii, K., Matsushita, H. and Miyazawa, Y., "Synthesis of Gust Load Alleviation with Flutter Margin Augmentation for a Transport Aircraft," Proceedings of the International Forum on Aeroelasticity and Structural Dynamics, Aachen, FRG, June 3-5, 1991, pp.474-480.

Table 1 GLA/FMA Performance of Control Laws

Control Law	Feed-back Variable	Order	GLA Analysis Strain Energy %	Control δa deg	Def. δe deg	GLA Experiment Bending Moment %	Accele-ration %	FMA Analysis Velocity Increment %	FMA Experiment Flutter Margin Increment
Full State			49	6.9	0.9			9.3	
A	a*	18	51	6.9	0.7			7.0	
AR	a	4	58	7.3	0.5	93	67	3.4	X 1.7
B	a/ε_B**	18	50	6.9	0.8			7.7	
BR	a/ε_B	2	68	6.1	0.4	80	69	4.9	X 1.5
C	a	18	61	6.8	0.4			18.1	
CR	a	2	78	5.6	1.1			12.0	
DR	a	2	80	5.2	0.9			11.0	

* a : Acceleration
** ε_B : Bending Strain
GLA : Gust Load Alleviation
FMA : Flutter Margin Augmentation

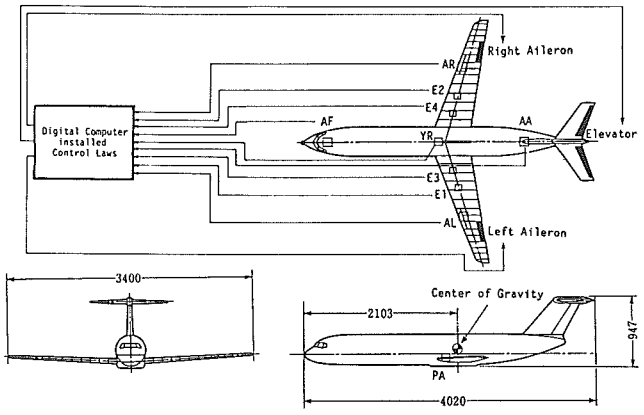

Fig.1 Aircraft Model Systematic Diagram

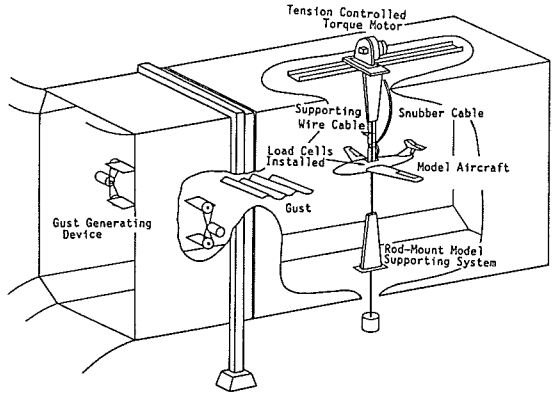

Fig.2 ACT Aircraft Model Wind Tunnel Test Set-up

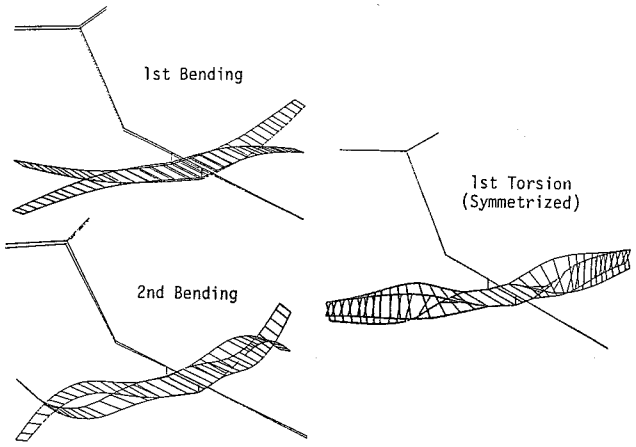

Fig.3 Aircraft Model Symmetrical Modes

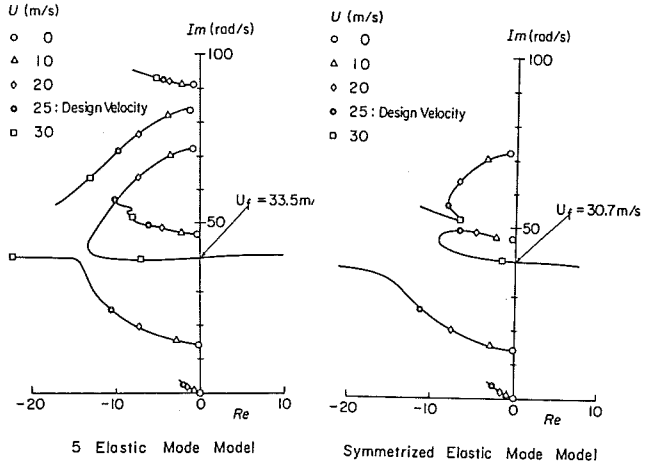

Fig.4 Velocity Root Locus

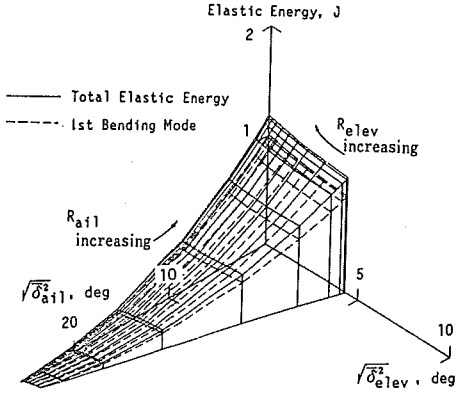

Fig.5 Energy vs Control Surface Deflection (U=25m/s)

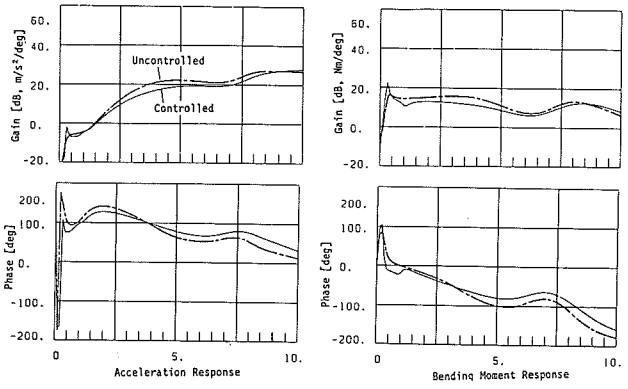

(1)Acceleration Feedback (AR)

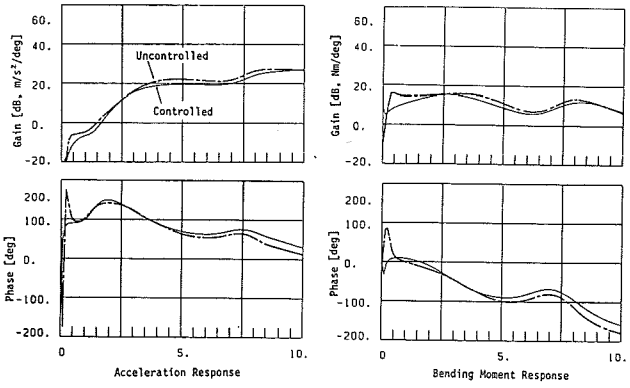

(2)Accel./Bending Strain Feedback (BR)

Fig.6 Frequency Response (Analysis)

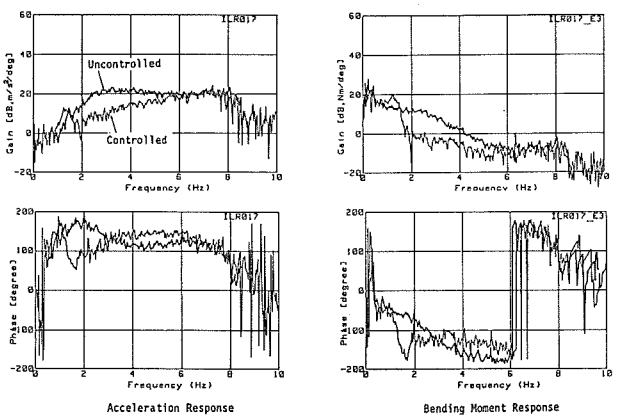

(1)Acceleration Feedback (AR)

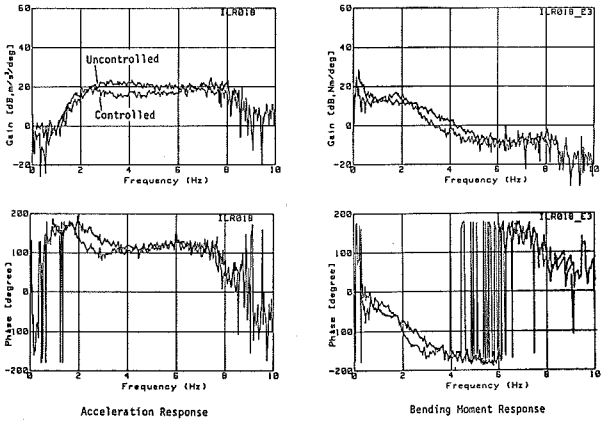

(2)Accel./Bending Strain Feedback (BR)

Fig.7 Frequency Response (Experiment)

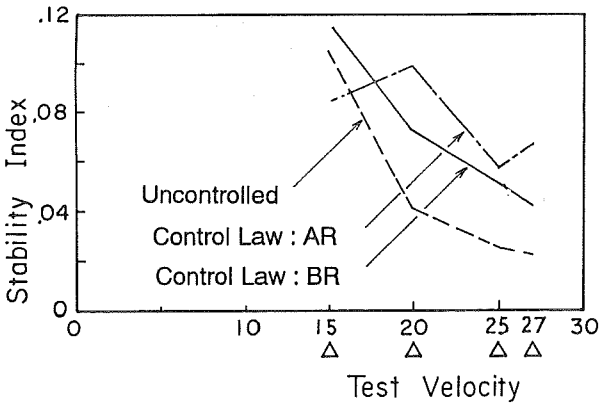

Fig.8 Flutter Margin (Experiment)

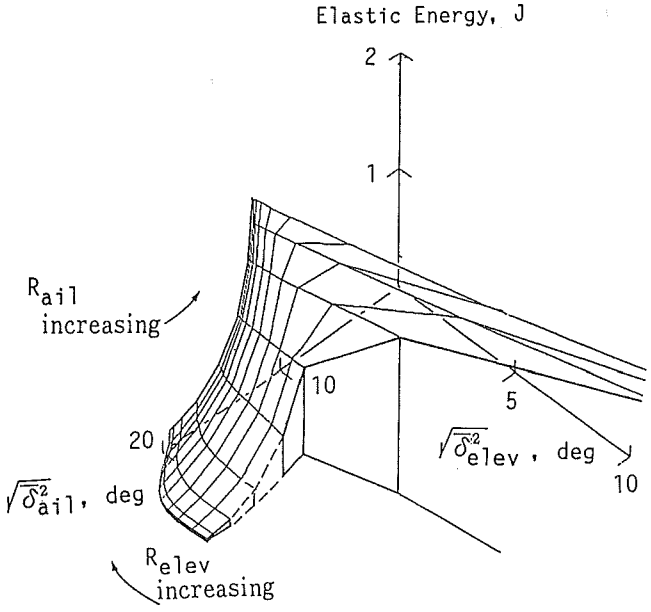

Fig.9 Energy vs Control Surface Deflection (U=33m/s)

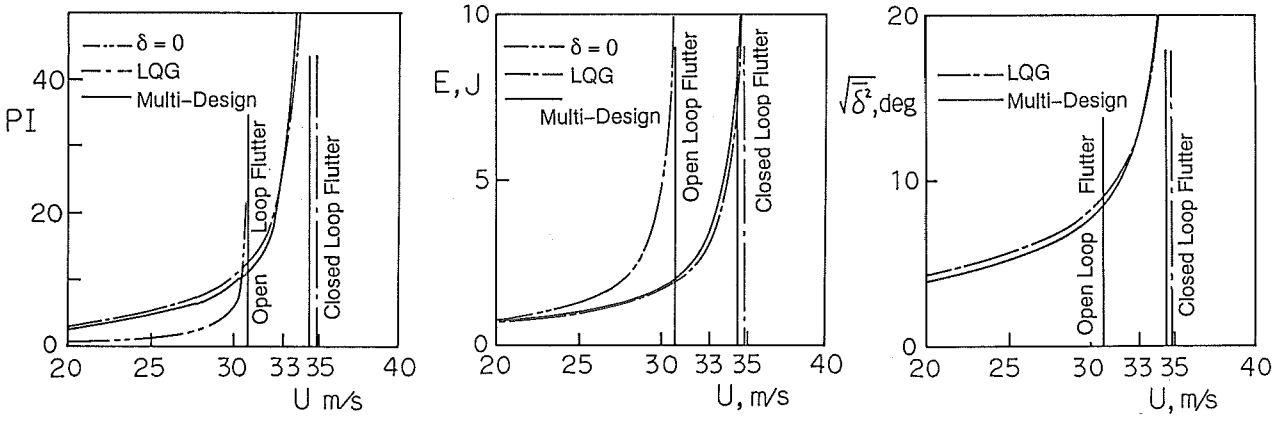

(a)Performance Index vs Velocity

(b)Elastic Energy vs Velocity

(c)Aileron Deflection vs Velocity

Fig.10 Control Law Performance vs Speed